Additive-Free Oxidative Cleavage of a Simple Lignin Model Compound in Air using Vanadium Complexes

Paul W. Musharbash,[†] Jerome B. Torres,[†] Tristhan Trieu-Tran, Peng Sun, S. Chantal E. Stieber, and Alex John*

Chemistry and Biochemistry Department
California State Polytechnic University, Pomona
3801 West Temple Ave., Pomona CA 91768.

Email: ajohn@cpp.edu

Graphical Abstract for Table of Contents

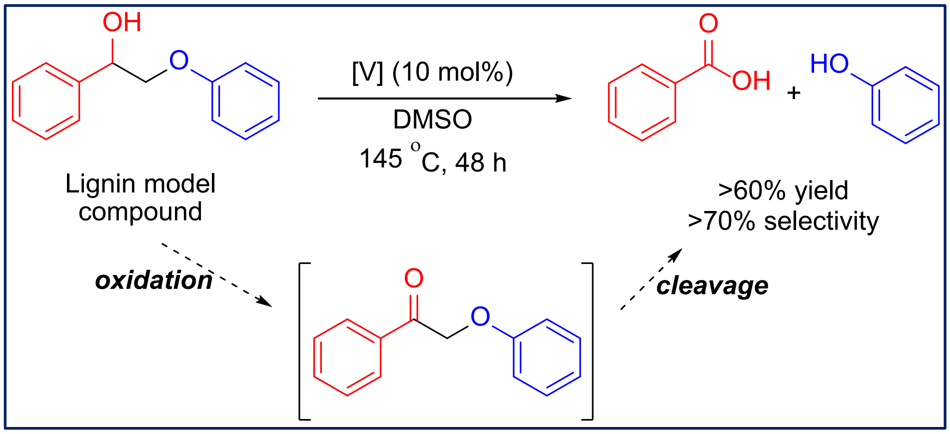

Abstract

Three vanadium complexes supported by salophan and salan ligands featuring differences in steric, electronic, and oxidation state (IV *vs* V) of the metal center have been evaluated for their potential in catalyzing the oxidative cleavage of a simple lignin model compound. All complexes were found to be effective, and under optimized conditions (145 ^{o}C, 48 h, in air) produced the cleavage products, phenol and benzoic acid, in good yields (62-69%) and selectivity (69-77%); significant differences in reactivity were not observed except at a lower temperature (125 ^{o}C). Complex **3c** featuring sterically bulky *tert*–butyl groups at *ortho*–/*para*– positions of the phenol arms, a cyclohexyl backbone and a V(V) center resulted in the highest yields and selectivity at 135 ^{o}C over 72 hours (69-78% yield; 78-89% selectivity). Longer reaction times as well as reaction temperatures were found to compromise yield and selectivity for both cleavage products. An oxidizing atmosphere was found to be crucial for the observed reactivity as reactions attempted under an inert atmosphere did not result in significant conversion. Preliminary mechanistic investigations suggest that the lignin model compound is oxidized prior to undergoing cleavage, and the vanadium(V) complex is more effective at cleaving the oxidized product in comparison to the vanadium(IV) counterparts. Quite significantly, the oxidative cleavage was achieved in the absence of basic or acidic additives.

Key Words

Lignin, Oxidative Cleavage, Vanadium, Catalysis, Ligands.

Introduction.

Lignocellulose is a byproduct of agricultural and forestry industry globally. It is non-edible and composed primarily of cellulose (40-80 %), hemicellulose (15-30 %) and lignin (15-30 %). Given the immense potential of lignocellulosic biomass to be a source for sustainable carbon (chemicals), the breakdown of its individual components to chemical feedstocks has received considerable attention in the recent past.[1–3] Lignin being a complex polymer with irregular structure, its utilization has met with limited success although it could be a sustainable source of renewable aromatics beyond the petrochemical era. About half of the lignin polymer found in biomass such as hardwood and softwood are composed of *β*-O-4 bonds, providing an ideal target for performing catalytic reactions focused on its depolymerization.[4, 5] Using either homogeneous or heterogenous catalysts several methods of catalytic depolymerization of lignin have been explored. Reaction types such as electrocatalysis,[6–8] photocatalysis,[9–14] oxidation,[15] reduction,[16, 17] redox,[18–20] and pyrolysis,[21, 22] etc. have been previously explored. Among these methods, oxidative cleavage has shown promise in efficient cleavage of *β*-O-4 and C_α-C_β bonds.

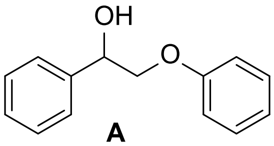

A

Figure 1. A simple *β*-O-4 lignin model compound.

Oxidative cleavage of lignin has been shown to offer multiple advantages over other methods as oxidation is the primary method used to break down lignin in nature and maintains much of the existing functionality in the polymer.[23] Multiple methods of carrying out oxidative cleavage reactions have been explored such as two-step oxidations which involve oxidation of the alcohol in lignin models to ketones before C_α-C_β bond cleavage.[24] Oxidative cleavage is typically achieved using transition metals catalysts such as iron,[17, 25] copper,[26–28] rhenium,[29] cobalt,[30] ruthenium,[31] and nickel.[32] Vanadium catalysis has received much interest due to its earth abundance compared to other rare and costly transition metals.[33–37] Both V(V) and V(IV) complexes have been previously explored in the oxidative cleavage of lignin model compounds.[7, 10, 23, 38–42] The identity of the metal center and the supporting ligand as well as solvent were found to have influence the selectivity of the cleavage as well as product composition. Prior studies involving vanadium complexes often involved the use of either basic or acidic additives for achieving effective catalysis.[23, 39, 43, 44]

The present study is focused on exploration of the effect of ligand structure and metal oxidation state on the oxidative cleavage reaction of a simple lignin model compound (**A**) catalyzed by vanadium complexes in the absence of acidic or basic additives (Figure 1).

Results and Discussion:

A. Synthesis and characterization of vanadium complexes: Ligands used for stabilizing the vanadium complexes evaluated in this study were synthesized by the reductive amination reaction starting with the corresponding salicylaldehyde and diamine (Scheme 1). The three ligands, $^{t\mathrm{Bu},t\mathrm{Bu}}\mathrm{L}_{\mathrm{Ph}}\mathrm{H}_2$ (**1b**), $^{\mathrm{H,H}}\mathrm{L}_{\mathrm{Ph}}\mathrm{H}_2$ (**2b**), and $^{t\mathrm{Bu},t\mathrm{Bu}}\mathrm{L}_{\mathrm{Cy}}\mathrm{H}_2$ (**3b**), feature differences in steric demand and backbone flexibility. While these ligands are known compounds,[45, 46] we report modified procedures that allowed the synthesis of these ligands in moderate to high yields (52–93%), especially **1b**.[47] All three ligands were satisfactorily characterized using infra-red (IR) and ^{1}H NMR spectroscopy (Figures S1-S9). The vanadium complexes, $^{t\mathrm{Bu},t\mathrm{Bu}}\mathrm{L}_{\mathrm{Ph}}\mathrm{VO}$ (**1c**), $^{\mathrm{H,H}}\mathrm{L}_{\mathrm{Ph}}\mathrm{VO}$ (**2c**),[46] and $(^{t\mathrm{Bu},t\mathrm{Bu}}\mathrm{L}_{\mathrm{Cy}}\mathrm{VO})_2\mathrm{O}$ (**3c**),[45] were synthesized in 50–87% yields from the corresponding ligands by reacting with the commercially available precursor, $\mathrm{VO(acac)}_2$.

Although a similar procedure was used for the synthesis of all three complexes, the reaction of **3b** with VO(acac)2 resulted in the oxidation of the vanadium(IV) center in the precursor and produced the *μ*-oxo dimer vanadium(V) complex **3c**, presumably *via* oxidation of an initial vanadium (IV) complex. Complex **3c** has been previously reported and was obtained during attempted recrystallization of the corresponding V(IV) complex in air.[45] The facile oxidation of the initial vanadium(IV) complex in case of **3c** under our reaction conditions could be the result of enhanced electron density on the vanadium center due to increased basicity of the cyclohexyl diamine backbone in **3b** as compared to the phenylene diamine backbone in **1b** and **2b**.

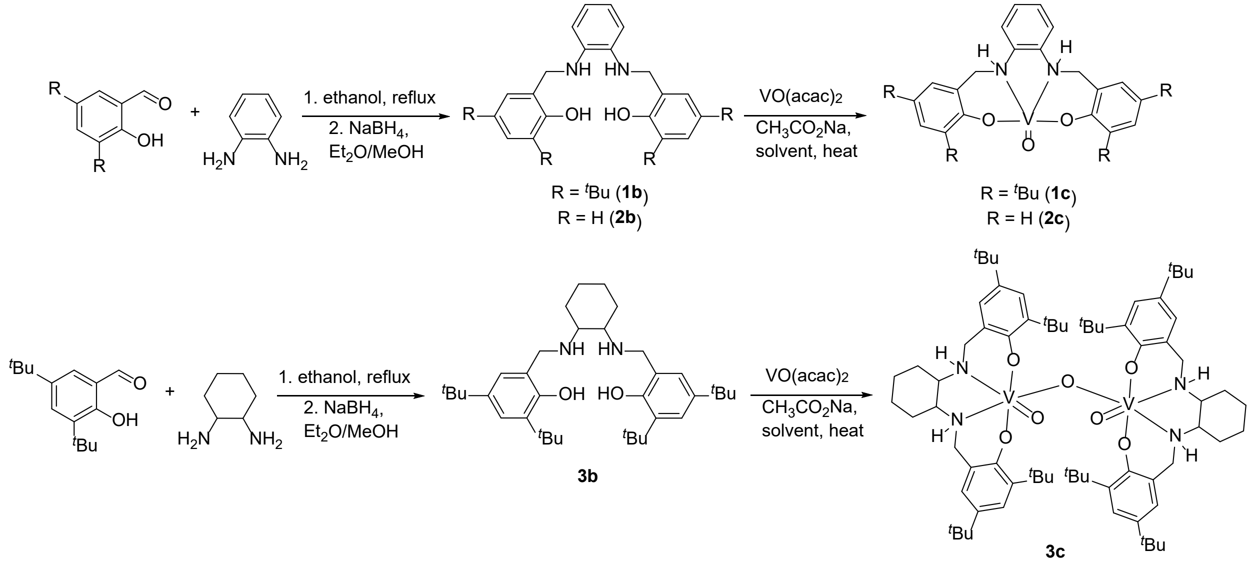

Scheme 1. Synthesis and structures of vanadium complexes (**1c–3c**) used in this study.

The synthesized vanadium complexes were successfully characterized using NMR spectroscopy (**3c**), IR spectroscopy, mass spectrometry, and elemental analysis. The IR spectrum of these complexes exhibited the characteristic V=O stretch at 973 cm^{-1} (**1c**), 974 cm^{-1} (**2c**), and 906 cm^{-1} (**3c**) which agree with literature ranges for the V=O bond in related compounds (Figures S10-S12).[48] The observed lower V=O stretch at 906 cm^{-1} for **3c** is in good agreement with the previous report.[45] The diamagnetic V(V) complex **3c** was also characterized by ^{1}H and $^{13}C\{^{1}H\}$ NMR spectroscopy; both spectra suggest an asymmetric coordination of the ligand to the metal center (Figures S13-S14). While successful mass spectrometry data (ESI+) could be obtained on complexes **2c** and **3c**, the molecular ion peak could not be detected for complex **1c**; only a probable fragment peak could be observed (Figures S15-S18). The oxidation state of the vanadium center in **1c**–**3c** was further confirmed using magnetic susceptibility measurements, electron paramagnetic resonance (EPR) spectroscopy, and UV-Vis spectrophotometry.[45, 49] Magnetic susceptibility measurements using Evan's method resulted in magnetic moments (μ_{eff}) typical for V(IV) centers (S=1/2) for complexes **1c** (1.72 B.M.) and **2c** (1.76 B.M.), while complex **3c** was determined to be diamagnetic in nature. Magnetic moment data were further corroborated by room temperature X-band EPR spectroscopy (Figure S19). Both **1c** and **2c** exhibited EPR spectra typical for S = ½ V(IV) systems while the spectra for the V(V) complex **3c** did not show a similar feature. Solution characterization of **1c**–**3c** using UV-Vis spectroscopy in CH_2Cl_2 displayed features relevant to a V(IV) center for **1c** & **2c**, while those expected for a V(V) center were observed for **3c**. Specifically, both **1c** and **2c** exhibited two weak absorptions characteristic of d–d transition (ε < 1000 M^{-1} cm^{-1}) at 885 nm ($d_{xy} \rightarrow d_{xz}, d_{yz}$) and ~550 nm ($d_{xy} \rightarrow d_{x^2-y^2}$). Spectrum of complex **3c** on the other showed a strong ligand-to-metal charge transfer (LMCT) absorption (ε = ~6300 M^{-1} cm^{-1}) at ~525 nm which can be attributed to a charge transfer from a phenolate 'O' $p\pi$-orbital to empty 3d orbitals on the vanadium(V) center. Cyclic voltammetry studies were attempted on 1mM solutions of **1c**–**3c** in CH_2Cl_2 using a glassy carbon electrode and Ag/AgCl reference electrode, and complex **2c** showed a reversible redox process with $E_{1/2}$ of 0.15 V which is attributed to a V(IV)/V(III) couple (Figures S21-S22). However, **1c** was found to be electrochemically inactive under the conditions used and only a weak oxidation or reduction peak was detected for **3c**. The peak-peak separation (anodic to cathodic peaks) was ~0.2V, which also suggests that the oxidation or reduction of **3c** is a slow process (reaction rate is small).

B. Catalysis Studies: Catalytic testing involving **1c**, **2c**, and **3c** (10 mol%) were undertaken using the simple lignin model compound 2-phenoxy-1-phenylethanol (**A**) [39] in DMSO-d_6 as solvent in a pressure tube (under air) while monitoring conversion (of model compound) and product yields (of benzoic acid and phenol) by ^{1}H NMR spectroscopy using 1,3,5-tri-*tert*-butylbenzene as an internal standard (Scheme 2 and Table 1). The generation of formic acid, which is also a product of the oxidative cleavage, was not tracked since it could not be reproducibly and quantitatively monitored. We began our studies by attempting trials under various conditions to find the optimal balance between reaction length, reaction temperature, conversion of the model compound, and product yields.

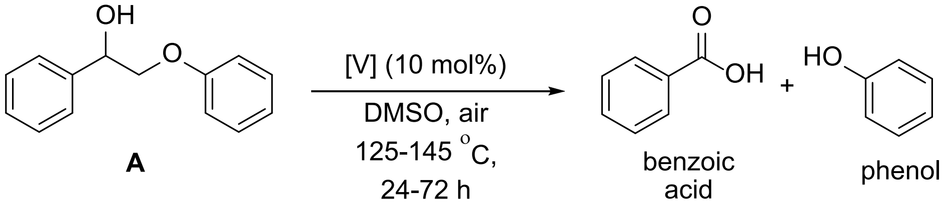

Scheme 2. Oxidative Cleavage of **A** catalyzed by complexes **1c**–**3c**.

Table 1. Oxidative Cleavage of a simple lignin model compound (**A)** catalyzed by vanadium complexes **1c**, **2c**, and **3c**.[a]

entry	**catalyst**	**T** (°C)	**time** (h)	**conversion** (%) (**A**)	**% yield (selectivity)**[b]	
					phenol	benzoic acid
1	**1c**	125	48	50	39 (78)	29 (58)
2		135	24	52	25 (48)	15 (29)
3			48	61	61 (100)	49 (80)
4			72	95	69 (73)	53 (56)
5		145	24	83	52 (63)	40 (48)
6			**48**	**90**	**64 (71)**	**69 (77)**
7			72	>99	68 (68)	64 (64)
8	**2c**	125	48	80	67 (84)	52 (65)
9		135	24	73	42 (57)	22 (30)
10			48	95	68 (71)	52 (55)
11			72	96	51 (53)	49 (51)
12		145	24	84	59 (70)	51 (61)
13			**48**	**90**	**62 (69)**	**69 (77)**
14			72	91	36 (39)	44 (48)
15	**3c**	125	48	81	59 (73)	57 (70)
16			72	94	64 (68)	56 (59)
17		135	24	66	37 (56)	33 (50)
18			48	90	67 (74)	60 (66)
19			**72**	**88**	**78 (89)**	**69 (78)**
20		145	24	84	49 (58)	42 (50)
21			**48**	**89**	**65 (73)**	**66 (74)**
22			72	93	30 (32)	57 (61)
23[c]		145	48	86	46 (53)	76 (88)
24	VO(acac)$_2$	145	48	63	43 (68)	25 (40)
25	VO(SO$_4$)	145	48	81	42 (52)	39 (48)
26	V$_2$O$_4$(acac)$_2$	145	48	100	68 (68)	54 (54)

[a] Reaction conditions: 0.12 mmol of **A** and 10 mol% catalyst in DMSO-d_6 (0.5 mL) in a sealed pressure reactor (under air) at varying temperatures using a heating block; reactions were run in duplicate (Table S1). [b] Yields were determined by ^{1}H NMR spectroscopy using 1,3,5-tri-*tert*-butylbenzene as an internal standard. [c] Using 5 mol% of **3c**.

Effect of reaction temperature: Catalytic runs at 125 ^{o}C for 48 hours (Table 1: entries 1, 8, and 15) yielded varying conversions across the three catalysts (**1c**: 50%, **2c**: 80%, **3c**: 81%). Complexes **2c** and **3c** produced higher yields of benzoic acid (**2c**: 52%, **3c**: 57%) than **1c** (29%). A similar trend was observed for phenol yields (**1c**: 39%, **2c**: 67%, **3c**: 59%) suggesting that **2c** and **3c** are more active at 125 ^{o}C. Increasing the temperature to 135 ^{o}C for 48 hours (Table 1: entries 3, 10, and 18) improved conversions for all three catalysts (**1c**: 61%, **2c**: 95%, **3c**: 90%). For **1c**, improvements in benzoic acid (49%) and phenol (61%) yields were also observed compared to the run at 125 ^{o}C, while yields stagnated or showed marginal improvements for **2c** and **3c** {benzoic acid (**2c**: 52%, **3c**: 60%) and phenol (**2c**: 68%, **3c**: 67%)}. Increasing the temperature to 145 ^{o}C (Table 1: entries 6, 13, and 21) further improved conversion of **A** for **1c** (90%) but showed marginal changes in conversion for **2c** (90%) and **3c** (89%). While these reactions at 145 ^{o}C all exhibited an improvement in the yield of benzoic acid (**1c**: 69%, **2c**: 69%, **3c**: 66%), the yield of phenol showed marginal improvement or even dropped (**1c**: 64%, **2c**: 62%, **3c**: 65%) when compared to the runs at 135 ^{o}C for 48 hours. The observed drop in phenol yields could be attributed to probable oxidation of phenol under the reaction conditions at elevated temperatures.

Effect of reaction time: Different reaction times across the same set of temperatures were evaluated next. Since low conversions were observed at 125 ^{o}C over 48 hours, a 24-hour reaction time was not explored at this temperature. Catalytic reactions were performed for 24 hours at 135 ^{o}C (Table 1: entries 2, 9, and 17) resulting in conversions of 52% for **1c**, 73% for **2c**, and 66% for **3c**. The lowest yields and selectivity for benzoic acid (**1c**: 15%, **2c**: 22%, **3c**: 33%) and phenol (**1c**: 25%, **2c**: 42%, **3c**: 37%) among all trials were obtained from the three catalysts under these conditions. Catalysis over 24 hours carried out at 145 °C (Table 1: entries 5, 12, and 20) however resulted in improved conversions (**1c**: 83%, **2c**: 84%, **3c**: 84%), benzoic acid (**1c**: 40%, **2c**: 51%, **3c**: 42%), and phenol (**1c**: 52%, **2c**: 59%, **3c**: 49%) yields for all catalysts in comparison to the run at 135 °C. A 72-hour reaction time was also explored at 135 °C and 145 °C. After the 72-hour period at 135 °C (Table 1: entries 4, 11, and 19), high conversions (**1c**: 95%, **2c**: 96%, **3c**: 88%) were observed for all three catalysts. However, benzoic acid (**1c**: 53%, **2c**: 49%, **3c**: 69%) and phenol yields (**1c**: 69%, **2c**: 51%, **3c**: 78%) did not show significant increases and in some cases showed a drop from trials at shorter time periods (48h). Catalyst **3c** based on a V(V) center showed the most consistent increase in yields for both products as the reaction time was increased from 24−72 hours at 135 °C [Figure 2(*a*)]. The most extreme conditions explored consisted of a 72-hour reaction time at 145 °C (Table 1: entries 7, 14, and 22 and Figure S23) where conversions marginally increased for all catalysts (**1c**: >99%, **2c**: 91%; **3c**: 93%) with marginal changes in yields of the products for all catalysts. All catalysts showed improvement in both benzoic acid and phenol yields when increasing reaction times from 24 hours to 48 hours at 145 °C, with **3c** showing the greatest improvement in yields for both products. Further increase in the reaction time to 72 hours resulted in significant loss in product yields for both **2c** [Figure 2(*b*)] and **3c**, while **1c** maintained yields like those observed at 48 hours. The observed decrease in product yield may be attributable to either decomposition or secondary reactions that may be occurring under the reaction conditions.[50, 51] For example, phenol could undergo oxidation or polymerization while benzoic acid can undergo decarboxylation.

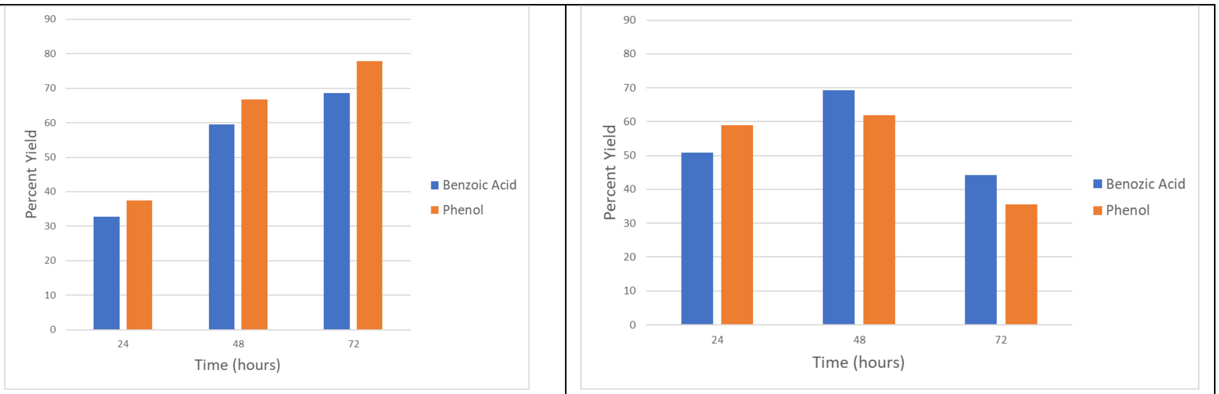

(*a*) Yields at 135 °C (24h *vs* 48h *vs* 72h) using **3c**.

(*b*) Yields at 145 °C (24h *vs* 48h *vs* 72h) using **2c**.

Figure 2. Effect of reaction time and temperature on product yield.

These optimization results indicate that the ideal balance for reaction conditions falls within the parameters of the conditions tested; 48-hour reaction time provided significant increases in catalytic yields across all tested temperatures. When temperatures were increased from 135 °C to 145 °C, **1c** and **2c** showed improved catalytic activity, with **3c** yields remained within error. A loss of product was observed for both **2c** and **3c** when reaction times were further increased to 72 hours, while **1c** remained unaffected. Overall, these time and temperature variations demonstrate that longer reaction times as well as high temperatures result in reduced selectivity for the cleavage products, and a combination of both was detrimental for the efficacy of the reaction. As a result of these studies, a 48-hour reaction time at 145 °C was identified as the optimal condition providing the best balance of reaction times and product yields with good selectivity. The effect of catalyst loading was tested using the V(V) complex **3c** (5 mol%) at 145 °C over 48 h (Table 1: entry 23); while a high yield (76%) and selectivity (88%) for benzoic acid are observed under these conditions, phenol yield (46%) and selectivity (53%) are lower for reasons that remain unclear. Readily accessible V(IV) and V(V) precursors, VO(acac)$_2$, VOSO$_4$ and V$_2$O$_4$(acac)$_2$, when tested for the oxidative cleavage of **A** under optimized conditions (Table 1: entries 24-26 and Figure S24), exhibited lower yields (25-68%) and selectivity (40-68%) for the cleavage products highlighting the superiority of complexes **1c**–**3c** in effecting the reaction. The V(V) precursor, $V_2O_4(acac)_2$, was found to be superior to its V(IV) precursor counterparts like the complex **3c** in comparison to **1c** and **2c**.

C. Mechanistic Studies: Having identified optimal conditions for the oxidative cleavage, further studies were subsequently undertaken to gain preliminary mechanistic insights into the oxidative cleavage catalyzed by these vanadium complexes (Table 2). A control run for 48 h with no added catalyst at 145 °C under air, produced the cleavage products phenol and benzoic acid in 8% and 4% yields respectively, although the conversion of **A** was 34% (Table 2: entry 1 and Figure S24). The low yields recorded in the control experiment suggest that the observed oxidative cleavage (Table 1) is indeed catalyzed by the vanadium complexes (**1c**–**3c**) used in this study, and thermal degradation of the model compound to the cleavage products is also possible although at a much slower rate and lower selectivity [phenol (23%) and benzoic acid (12%)]. Control reactions were next carried out using **1c**–**3c** (10 mol%) at 145 °C for 48 hours in a nitrogen flushed environment to understand the role of air (oxygen). Reactions carried out using V(IV) complexes, **1c** and **2c**, produced phenol [17% (**1c**); 19% (**2c**)] and benzoic acid [4% (**1c**); 8% (**2c**)] in significantly lower yields (Table 2: entries 2 and 3) compared to catalytic reactions carried out under air (Table 1: entries 6 and 13). A similar reaction carried out using the V(V) complex **3c** showed incomplete conversion of the model compound (58%) and the oxidation product (ketone **B)** was observed (12%) in addition to phenol (22%) and benzoic acid (8%) (Table 2: entry 4 and Figure S25). The ketone **B** was not detected using **1c** and **2c**. These results (Table 2: entries 1-4) are suggestive of the ketone being an intermediate prior to cleavage under the reaction conditions and the need for an oxidant (such as oxygen in air) for efficient turnover. This observation is supported by previous studies which note that oxygen is not required for achieving turnover but catalytic activity is significantly reduced under anaerobic conditions.[52]

To validate the intermediacy of the ketone **B** in the reaction, we performed additional studies using **B** as the substrate (Table 2: entries 5-10). When **B** was used as substrate in a catalytic reaction (10 mol% **2c** or **3c**, 145 ^{o}C, 48h) under N_2 atmosphere, a partial conversion (**2c**: 76%; **3c**: 68%) to phenol (**2c**: 40%; **3c**: 39%) and benzoic acid (**2c**: 29%; **3c**: 52%) was observed (Table 2: entries 5 and 6). A reaction under air resulted in 52% conversion of the ketone within 4 hours using **2c** producing phenol and benzoic acid in 41% and 23% yields respectively (Table 2: entry 7). Extending the reaction time to 16 hours under these conditions yielded phenol and benzoic acid in 73% and 43% yields respectively at complete conversion (Table 2: entry 8). Similar studies using the V(V) complex **3c** resulted in complete conversion of **B** within 4 hours, producing phenol (84%) and benzoic acid (54%) while extending the reaction time to 24 hours resulted in a drastic drop in phenol yield (28%) while benzoic acid yield was practically unchanged (57%); presumably due to further oxidation of phenol to unidentified oxidation products under these conditions (Table 2: entries 9 and 10). Cumulatively, these studies highlight the need for a terminal oxidant, presumably oxygen from ambient air, to facilitate the cleavage reaction, and the intermediacy of the ketone during the catalytic process (oxidation followed by cleavage). Furthermore, the V(V) complex **3c** was found to be more effective than the V(IV) complex **2c** is cleaving the ketone intermediate (Table 2: entries 7 and 9).

Table 2. Oxidative Cleavage of model compound (**A**) and ketone (**B**)catalyzed by vanadium complexes.[a]

entry	**substrate**	**catalyst**	**time** (h)	**conversion** (%)	% **yield** (**selectivity**)[b]	
					phenol	benzoic acid
1[c]	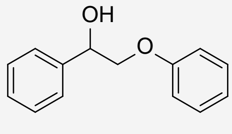 **A**	-	48	34	8 (23)	4 (12)
2[d]		**1c**	48	28	17 (61)	4 (14)
3[d]		**2c**	48	40	19 (47)	8 (20)
4[d,e]		**3c**	48	58	22 (38)	8 (14)
5[d]	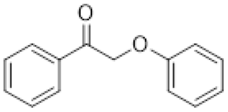 **B**	**2c**	48	76	40 (53)	29 (38)
6[d]		**3c**	48	68	39 (57)	52 (76)
7[c]		**2c**	4	52	41 (79)	23 (44)
8[c]		**2c**	16	100	73 (73)	43 (43)
9[c]		**3c**	4	100	84 (84)	54 (54)
10[c]		**3c**	24	100	28 (28)	57 (57)

[a] Reaction conditions: 0.12 mmol of **A** and 10 mol% catalyst in DMSO-d_6 (0.5 mL) in a sealed pressure reactor at 145 °C using a heating block. [b] Yield and selectivity were determined by ^{1}H NMR spectroscopy using 1,3,5-tri-*tert*-butylbenzene as an internal standard. [c] Reaction under air. [d] Reaction under N_2 atmosphere. [e] Ketone **B** was formed in 12% yield in addition to phenol (22%) and benzoic acid (8%).

To ascertain the intermediacy of the ketone **B** in the oxidative cleavage reaction, a time dependence study was attempted in an NMR tube at 135 °C using **2c** (10 mol%). Very little conversion of the model compound **A** was observed in the first 12 hours (time dependence) of the reaction, with a 24-hour analysis showing similar results. We hypothesized that this could be due to limited amount of headspace as well as solution interface that was in contact with the headspace in the NMR tube as opposed to our regular catalytic reactions (in 0.5 mL solvent) carried out in pressure tubes (*ca*. 35 mL). Hence, we conducted the time dependence study using our regular setup by analyzing the sample at regular intervals using ^{1}H NMR spectroscopy (Figure 3). The acquired spectra were compared to those of standard samples (benzoic acid, phenol, ketone **B**, and model compound **A**) to track the progress of the reaction. This study clearly demonstrates that the lignin model compound is initially oxidized to the ketone (1–4 hours) without any significant amount of cleavage products. However, at the 24-hour mark, a significant amount of the cleavage products is observed with a concomitant decrease in the amount of the ketone **B**. The model compound and the ketone are almost completely converted within 48 hours. This time dependence experiment corroborates our findings from earlier that the lignin model is first oxidized to the ketone before undergoing cleavage to form benzoic acid and phenol.

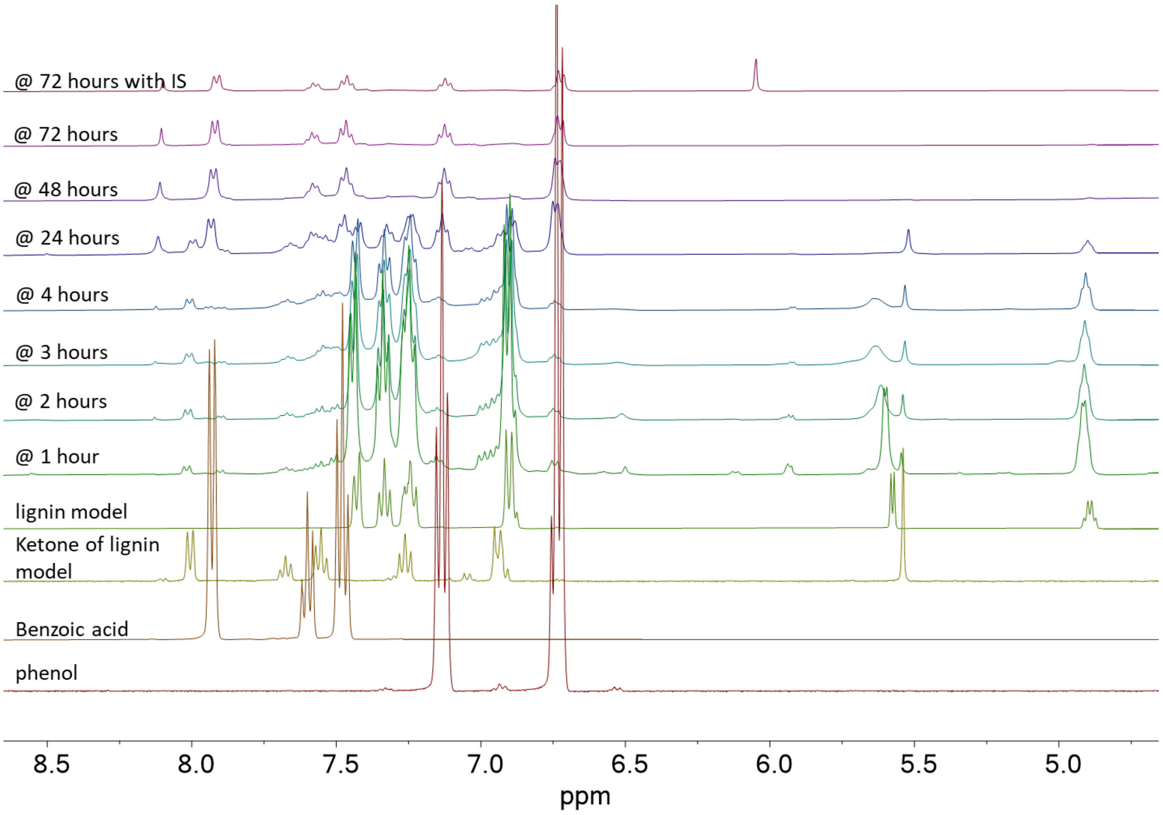

Figure 3. Time dependence of the oxidative cleavage of lignin model using **2c**.

The catalytic activity of **1c**–**3c** in the oxidative cleavage of **A** cannot be directly compared to previous studies involving vanadium catalysts since the use of acidic and/or basic additives or solvent usually allows the catalysis to be performed under milder conditions. For example, Xu *et al* demonstrated that oxidative cleavage of **A** using 10 mol% V(IV) precursors such as $VO(acac)_2$

and $VO(OAc)_2$ (80 °C, 8 h, 1 atm O_2) resulted in an improved conversion of **A** from <2% to 76% in presence of CH_3COOH (AcOH) as solvent.[39] The conversion of the model compound was just 16% using DMSO as a solvent while it increased to >90% when acids were used as solvents. Additionally, the use of AcOH as a solvent instead of CH_3CN switched the selectivity of reaction from C–H oxidation to C–C cleavage. High conversions were maintained (89%) even when 10% AcOH in CH_3CN was used as solvent; benzoic acid and phenol were formed in 29% and 44% yields respectively under these conditions. Thorn and coworkers demonstrated that a V(V) complex (dipic)VO(O^iPr) could catalyze the cleavage of **A** to benzoic acid (81%), phenol (77%), and formic acid (46%) in DMSO-d_6 at 100 °C but required 7 days to reach 95% conversion.[42] Similarly, Jones and coworkers studied a series of V(V) complexes supported by tridentate Schiff-base ligands to elucidate ligand effects in the oxidative cleavage of **A** (DMSO, 100 °C, 4 days). Ligands featuring electron-withdrawing halogen substituents favored oxidation while those featuring alkyl substituents resulted in enhanced selectivity for C-O cleavage.[52] Similar studies at lower temperatures (80-100 °C) usually need longer reaction times to reach high conversions while using **1c**–**3c** high conversions and selectivity can be achieved in 48 hours although at a higher temperature (145 °C).

Conclusion

In summary, we have investigated the oxidative cleavage of a simple lignin model compound using vanadium complexes of salan and salophan ligands. Catalytic reactions were optimized to produce the cleavage products in good yields (60-70%) at 145 °C in 48 hours in the absence of basic or acidic additives. Significant differences in catalytic activity were not observed between the three complexes except at longer reaction times (72h) at high temperatures (135 or 145 °C) when catalyst

1c was found to maintain high selectivity. The phenol product was found to undergo secondary reactions that resulted in decreased yield and selectivity at prolonged times and high reaction temperatures. Preliminary mechanistic studies show that the lignin model compound is oxidized prior to undergoing cleavage and the vanadium(V) complex **3c** is superior at effecting the cleavage of the ketone intermediate. Further mechanistic investigations involving vanadium(IV/V) complexes displaying steric and electronic modulation are currently underway in our laboratory.

Acknowledgments

Funding for this work was provided by the California State University–Agricultural Research Institute (CSU-ARI # 20-04-121). AJ would also like to acknowledge support from the U.S. National Science Foundation (NSF), grant number CHE-1800605 as well as the Chemistry & Biochemistry Department & College of Science at California State Polytechnic University, Pomona. S.C.E.S. thanks the California State University Agricultural Research Institute (21-04-108), NSF CAREER (1847926), and the Camille & Henry Dreyfus Foundation for funding. AJ would like to thank the UCI Mass Spectrometry Facility (Dr. Felix Grun and Mr. Chris Dickson) for assistance with small molecule analyses and accurate mass measurements.

Author Contributions

AJ developed the research idea; PWM, JBT, TT, and AJ performed the experimental work including synthesis and characterization of ligands/vanadium complexes as well as catalytic studies; PS helped with collecting and analyzing CV data; SCES helped with collecting and analyzing EPR data; PWM, JBT, and AJ wrote the manuscript. PWM and JBT contributed equally and should be considered co-first authors.

Experimental Section

General Procedures: All air and water sensitive manipulations were carried out under a nitrogen atmosphere by using standard pressure reactors. All ^{1}H NMR spectra were collected on a Varian 400-MR spectrometer. Chemical shifts (δ) for ^{1}H NMR spectra were referenced to the residual protons on deuterated chloroform (7.26 ppm) and deuterated dimethyl sulfoxide (2.5 ppm). Infrared spectra were recorded on a Thermo Scientific NICOLET iS10 Spectrophotometer equipped with a SMART iTR. Elemental analysis was performed at Robertson Microlit Laboratories (New Jersey, USA). Precursors for ligand and complex synthesis were used as received. $CDCl_3$ was used as received from Sigma. Solvents (ethanol, toluene, dichloromethane, and hexanes) were purchased from Fisher Scientific and used as received. All starting materials were procured from commercial sources and used without further purification. EPR data were measured using a Magnettech MS 5000 benchtop EPR/ESR spectrometer. Sample solutions were transferred to capillaries and sealed with Cryoseal for measurements. Magnetic moment data were collected using a Sherwood Scientific Magnetic Susceptibility Balance model MK1. ESI-MS data were collected on a Waters LCT Premier by flow injection analysis (FIA) in methanol and data analyzed with MassLynx v. 4.1 software. In ESI+ mode, analyte m/z ions (M+H)+ or (M+Na)+ were validated to less than ± 5 ppm relative to the nearest sodiated polyethylene glycol (CAS: 25322-68-3, av. Mwt 400)) or sodiated methoxypolyethyleneglycol (CAS: 990-74-4, av. Mwt 350) calibrant peak lockmass. UV-Vis spectra were collected using an Agilent Cary 60 UV-Vis spectrophotometer in CH_2Cl_2.

Synthesis of Ligands

Synthesis of 1a: A round bottom flask was charged with 3,5-di-*tert*-butyl-salicilaldehyde (2.00g, 8.58 mmol) and (0.466g, 4.32 mmol) of 1,2-phenylenediamine were added into ethanol (*ca*. 30 mL). The solution was refluxed 48 hours, turning from an initial pale-yellow color to a bright orange color at the completion of the reaction. The resulting solution was allowed to cool, and the precipitate was filtered out of the solvent via gravity filtration. The precipitate was then allowed to air dry, and the dry, yellow product was weighed. (2.04g, 87%): ^{1}H NMR ($CDCl_3$, 400 MHz, 28 °C) δ = 8.66 (s, 2H), 7.44 (d, 2H, $^4J_{HH}$ = 2Hz), 7.32-7.22 (m, 6H), 7.20 (d, 2H, $^4J_{HH}$ = 3Hz), 1.44 (s, 18H), 1.32 (s, 18H).

Synthesis of 2a: To a round bottom flask was added 1,2-phenylenediamine (0.234g, 2.16 mmol), salicylaldehyde (0.444mL, 4.25 mmol), and ethanol (*ca*. 10 mL). The mixture was stirred, and the solution will initially be a yellow-green color and will turn to a yellow-orange color in a few minutes. The solution was then placed on a moderate reflux for 24 hours and a yellow precipitate formed. The precipitate was gravity filtered and obtained as a yellow powder after drying on a high vacuum. (0.58g, 83%): ^{1}H NMR ($CDCl_3$, 400 MHz, 29°C) δ = 8.64 (s, 2H), 7.40-7.33 (m, 6H), 7.27-7.23 (m, 2H), 7.06 (d, 2H, $^3J_{HH}$ = 8Hz), 6.92 (t, 2H, $^3J_{HH}$ = 8Hz).

Synthesis of 3a: To a round bottom flask was added 3,5-di-*tert*-butyl-salicylaldehyde (1.99g, 8.49 mmol), 1,2-cyclohexanediamine (0.51mL, 4.25 mmol), and ethanol (*ca*. 15 mL). The mixture was placed on a reflux and within 5 minutes, the yellow solution started to thicken. Additional ethanol (*ca*. 15 mL) was added, and the reaction was refluxed for 24 hours to form a yellow precipitate. The precipitate was gravity filtered and washed with cold methanol. The product was obtained as a bright, yellow powder after drying on a high vacuum. (2.07g, 89%): ^{1}H NMR ($CDCl_3$, 400 MHz, 29°C) δ =8.29 (s, 2H), 7.29 (d, 2H, $^4J_{HH}$ = 2Hz), 6.98 (d, 2H, $^4J_{HH}$ = 3Hz), 3.31 (d, 2H, $^4J_{HH}$ = 3Hz), 1.96-1.86 (m, 4H), 1.75-1.72 (m, 2H), 1.52-1.45 (m, 4H), 1.41 (s, 18H), 1.23 (s, 18H).

Synthesis of 1b: To a round bottom flask, ligand **1a** (1.00g, 1.85 mmol) and $NaBH_4$ (1.05 g, 2.79 mmol) were added to a solution of diethyl ether (*ca*. 30 mL) and methanol (*ca*. 10 mL). The reaction was allowed to stir for 1 hour, starting as a yellow color. Over the course of the hour, the diethyl ether evaporated out of the solution, depositing a white precipitate on the walls of the flask. The remaining contents were purified by an aqueous workup (*ca*. 10 mL) where the organic compound was insoluble. The precipitate was collected *via* gravity filtration and dried on a high vacuum to obtain **1b** as a white powder. (0.95g, 93%): ^{1}H NMR ($CDCl_3$, 400 MHz, 28°C) δ = 7.28 (s, 2H), 7.05 (s, 2H), 6.99 (s, 4H), 4.37 (s, 4H), 1.39 (s, 18H), 1.30 (s, 18H). IR (thin film, cm^{-1}) υ(N-H) = 3279, υ(C_{sp^3}-H) = 2952, 2865, and υ(C-O) = 1230.

Synthesis of 2b: To a round bottom flask, ligand **2a** (0.500g, 1.58 mmol) and $NaBH_4$ (0.717g, 18.96 mmol) were added to a solution of diethyl ether (*ca*. 30 mL) and methanol (*ca*. 10 mL). The reaction mixture was stirred at room temperature until the yellow solution changed to colorless. The solution was transferred into a separatory funnel. DI H_2O (*ca*. 10 mL) was added, and the mixture was extracted along with ethyl acetate (*ca*. 7 mL), diethyl ether (*ca*. 7 mL), and dichloromethane (*ca*. 7 mL). The organic layer was dried using Na_2SO_4 and filtered. The filtrate was concentrated on the rotary evaporator as a light-brown oil and dried under high vacuum as a tan powder. (0.44g, 86%): ^{1}H NMR (DMSO-d_6, 400 MHz, 27°C) δ = 9.48 (s, 2H), 7.18 (d, 2H, $^3J_{HH}$ = 8Hz), 7.03 (t, 2H, $^3J_{HH}$ = 8Hz), 6.80 (d, 2H, $^3J_{HH}$ = 8Hz), 6.71 (t, 2H, $^3J_{HH}$ = 8Hz), 6.45-6.37 (m, 4H), 5.01 (t, 2H, $^3J_{HH}$ = 8Hz), 4.21 (d, 4H, $^3J_{HH}$ = 8Hz). IR (thin film, cm^{-1}) υ(N-H) = 3286 and υ(C-O) = 1235.

Synthesis of 3b: To a round bottom flask, ligand **3a** (1.00g, 1.87 mmol) and $NaBH_4$ (1.03g, 27.2 mmol) were added to a solution of diethyl ether (*ca*. 20 mL). The reaction mixture was stirred at room temperature for 0.5 hours. After 0.5 hours, methanol (*ca*. 20 mL) was added to the solution and the mixture was stirred for an additional 1.5 hours, until the yellow solution turned colorless. The solution was transferred into a separatory funnel. DI H_2O (*ca*. 10 mL) was added, and the mixture was extracted along with ethyl acetate (*ca*. 7 mL), diethyl ether (*ca*. 7 mL), and dichloromethane (*ca*. 7 mL). The organic layer was dried using Na_2SO_4 and filtered. The filtrate was concentrated on the rotary evaporator and dried under high vacuum as a white powder. (0.53g, 52%): ^1H NMR (DMSO-d_6, 400 MHz, 27°C) $\delta = 7.03$ (d, 2H, $^4J_{HH} = 2Hz$), 6.87 (d, 2H, $^4J_{HH} = 3Hz$), 3.93-3.78 (m, 4H), 2.44 (s, 2H), 1.98 (d, 2H, $^4J_{HH} = 3Hz$), 1.61 (s, 2H), 1.31 (s, 18H), 1.21 (s, 18H), 1.18-1.14 (m, 2H). IR (thin film, cm^{-1}) $\upsilon(C_{sp^3}\text{-}H) = 2950, 2865$ and $\upsilon(C\text{-}O) = 1235$.

Synthesis of 1c: To a round bottom flask, ligand **1b** (0.300g, 0.547 mmol), sodium acetate (0.133g, 0.979 mmol), and $VO(acac)_2$ (0.149g, 0.563 mmol) was added to a toluene solution (*ca*. 7 mL). The mixture was refluxed for 24 hours, initially turning into a dark-green color. The dark solution was concentrated on a rotary evaporator until a suspension formed and was filtered. The precipitate was washed with cold dichloromethane and dried under high vacuum to obtain a yellow-green powder. (0.205g, 62%): IR (thin film, cm^{-1}) $\upsilon(C_{sp^3}\text{-}H) = 2948, 2862$, $\upsilon(C\text{-}O) = 1250$, and $\upsilon(V{=}O) = 973$. Anal. Calcd. for $C_{37}H_{53}N_2O_3V{\bullet}3CH_2Cl_2$: C, 54.62 %; H, 6.76 %; N, 3.18 %. Found: C, 55.15 %; H, 5.91 %; N, 2.51 %. $\mu_{eff} = 1.72$ B.M. ESI-MS+: 628.5 $[(LVO)+CH_3OH-28]^+$. UV-Vis (CH_2Cl_2; λ_{max} (nm), ε (M^{-1} cm^{-1})): 885, 116; 590, 220.

Synthesis of 2c: To a round bottom flask, ligand **2b** (0.314g, 0.981 mmol), sodium acetate (0.143g, 1.75 mmol), and $VO(acac)_2$ (0.267g, 1.01 mmol) was added to a toluene solution (*ca*. 7 mL). The dark-green mixture was refluxed for 6 hours. The dark solution was concentrated on a rotary evaporator until a suspension formed and was filtered. The precipitate was washed with cold dichloromethane and dried under high vacuum to obtain a dark green solid. (0.329g, 87%): IR (thin film, cm^{-1}) υ(C-O) = 1258, and υ(V=O) = 973. Anal. Calcd. for $C_{20}H_{18}N_2O_3V•CH_2Cl_2•H_2O$: C, 51.66 %; H, 4.54 %; N, 5.74 %. Found: C, 51.18 %; H, 4.12 %; N, 3.56 %. μ_{eff} = 1.76 B.M. HRMS (ESI/Q-TOF) *m/z*: $[M+CH_3OH]^+$ Calcd. for $[C_{20}H_{18}N_2O_3V•CH_3OH]^+$ 417.1019; Found 417.0002. UV-Vis (CH_2Cl_2; λ_{max} (nm), ε (M^{-1} cm^{-1})): 885, 83; 540, 950.

Synthesis of 3c: To a round bottom flask, ligand **3b** (0.249g, 0.453 mmol), sodium acetate (0.067g, 0.811 mmol), and $VO(acac)_2$ (0.124g, 0.467 mmol) was added to an ethanol solution (*ca*. 7 mL). The mixture was refluxed for 24 hours as a dark-purple color. The solution was concentrated on a rotary evaporator and was filtered. The precipitate was washed with cold dichloromethane and dried under high vacuum to obtain a dark purple powder. (0.141g, 50%): ^1H NMR ($CDCl_3$, 400 MHz, 28°C) δ = 7.21 (d, 1H, $^4J_{HH}$ = 2 Hz), 7.19 (d, 1H, $^4J_{HH}$ = 2 Hz), 6.90 (d, 1H, $^4J_{HH}$ = 4 Hz), 6.64 (d, 1H, $^3J_{HH}$ = 8 Hz), 6.52 (d, 1H, $^4J_{HH}$ = 2 Hz), 5.99 (d, 1H, $^2J_{HH}$ = 16 Hz), 4.37 (d, 1H, $^2J_{HH}$ = 12 Hz), 3.74 (t, 1H, $^2J_{HH}$ = 12 Hz), 3.42 (d, 1H, $^2J_{HH}$ = 12 Hz), 3.16-3.08 (m, 1H), 2.48-2.41 (m, 1H), 2.30-2.20 (m, 2H), 1.70-1.59 (m, 4H), 1.54 (s, 9H), 1.28 (s, 9H), 1.27 (s, 9H), 1.21 (s, 9H), 1.16-1.05 (m, 2H), 0.75-0.73 (m, 1H). $^{13}C\{^1H\}$ NMR ($CDCl_3$, 100 MHz, 28°C) δ = 162.1, 160.1, 143.0, 139.3, 135.2, 134.7, 125.4, 123.8, 123.7, 122.6, 122.4, 119.0, 61.1, 61.0, 54.0, 49.2, 35.4, 35.3, 34.3, 34.1, 31.7, 31.5, 31.0, 30.9, 30.7, 29.2, 24.3, 24.1. IR (thin film, cm^{-1}) υ($C_{sp}{}^3$-H) = 2950, 2865, υ(C-O) = 1235, υ(V=O) = 906. Anal. Calcd. for $C_{74}H_{118}N_4O_7V_2•2CH_2Cl_2•2H_2O$: C, 61.53 %; H, 8.56 %; N, 3.78 %. Found: C, 61.75 %; H, 8.30 %; N, 3.79 %. μ_{eff} = 0.17 B.M. HRMS

(ESI/Q-TOF) *m/z*: $[M+K]^+$ Calcd. for $[C_{37}H_{59}N_2O_3V{\bullet}K]^+$ 669.3602; Found 669.3602. UV-Vis (CH_2Cl_2; λ_{max} (nm), ε (M^{-1} cm^{-1})): 525, 6284.

Representative procedure for catalysis reactions.

Lignin model compound (0.12 mmol) and 10 mol% catalyst (**1c**, **2c** or **3c**) along with DMSO-d_6 (0.5 mL) were loaded into a sealed pressure reactor (under air) and heated in a heating block for the requisite amount of time. At the end of run, 1,3,5-tri-tert-butylbenzene (internal standard) dissolved in $CDCl_3$ (*ca*. 0.5 mL) was added into the reaction mixture. The mixture was then analyzed by ^1H NMR spectroscopy to quantify conversion and yield. It was necessary to use a mixture of DMSO-d_6 and $CDCl_3$ for the analysis since the internal standard has poor solubility in DMSO-d_6.

References

1. Sudarsanam P, Duolikun T, Babu PS, et al (2020) Recent developments in selective catalytic conversion of lignin into aromatics and their derivatives. Biomass Conv Bioref 10:873–883. https://doi.org/10.1007/s13399-019-00530-1

2. Guadix-Montero S, Sankar M (2018) Review on Catalytic Cleavage of C–C Inter-unit Linkages in Lignin Model Compounds: Towards Lignin Depolymerisation. Top Catal 61:183–198. https://doi.org/10.1007/s11244-018-0909-2

3. Sun Z, Fridrich B, De Santi A, et al (2018) Bright Side of Lignin Depolymerization: Toward New Platform Chemicals. Chem Rev 118:614–678. https://doi.org/10.1021/acs.chemrev.7b00588

4. Zhang Z, Yin G, Andrioletti B (2022) Advances in value-added aromatics by oxidation of lignin with transition metal complexes. Transit Met Chem 47:189–211. https://doi.org/10.1007/s11243-022-00498-4

5. Zhang C, Wang F (2020) Catalytic Lignin Depolymerization to Aromatic Chemicals. Acc Chem Res 53:470–484. https://doi.org/10.1021/acs.accounts.9b00573

6. Yang C, Maldonado S, Stephenson CRJ (2021) Electrocatalytic Lignin Oxidation. ACS Catal 11:10104–10114. https://doi.org/10.1021/acscatal.1c01767

7. Ma L, Zhou H, Kong X, et al (2021) An Electrocatalytic Strategy for C–C Bond Cleavage in Lignin Model Compounds and Lignin under Ambient Conditions. ACS Sustainable Chem Eng 9:1932–1940. https://doi.org/10.1021/acssuschemeng.0c08612

8. Chang X, Van Der Zalm J, Thind SS, Chen A (2020) Reprint of "Electrochemical oxidation of lignin at electrochemically reduced TiO2 nanotubes." Journal of Electroanalytical Chemistry 872:114528. https://doi.org/10.1016/j.jelechem.2020.114528

9. Wang X, Chu S, Shao J, et al (2022) Efficient and Selective C–C Bond Cleavage of a Lignin Model Using a Polyimide Photocatalyst with High Photooxidation Capability. ACS Sustainable Chem Eng 10:11555–11566. https://doi.org/10.1021/acssuschemeng.2c02991

10. Liu H, Li H, Luo N, Wang F (2020) Visible-Light-Induced Oxidative Lignin C–C Bond Cleavage to Aldehydes Using Vanadium Catalysts. ACS Catal 10:632–643. https://doi.org/10.1021/acscatal.9b03768

11. Chen C, Liu P, Xia H, et al (2020) Photocatalytic Cleavage of β-O-4 Ether Bonds in Lignin over Ni/TiO2. Molecules 25:2109. https://doi.org/10.3390/molecules25092109

12. Nguyen ST, Murray PRD, Knowles RR (2020) Light-Driven Depolymerization of Native Lignin Enabled by Proton-Coupled Electron Transfer. ACS Catal 10:800–805. https://doi.org/10.1021/acscatal.9b04813

13. Wang Y, Liu Y, He J, Zhang Y (2019) Redox-neutral photocatalytic strategy for selective C–C bond cleavage of lignin and lignin models via PCET process. Science Bulletin 64:1658–1666. https://doi.org/10.1016/j.scib.2019.09.003

14. Luo N, Wang M, Li H, et al (2016) Photocatalytic Oxidation–Hydrogenolysis of Lignin β-O-4 Models via a Dual Light Wavelength Switching Strategy. ACS Catal 6:7716–7721. https://doi.org/10.1021/acscatal.6b02212

15. Luo H, Wang L, Li G, et al (2018) Nitrogen-Doped Carbon-Modified Cobalt-Nanoparticle-Catalyzed Oxidative Cleavage of Lignin β-O-4 Model Compounds under Mild Conditions. ACS Sustainable Chem Eng 6:14188–14196. https://doi.org/10.1021/acssuschemeng.8b02802

16. Feghali E, Carrot G, Thuéry P, et al (2015) Convergent reductive depolymerization of wood lignin to isolated phenol derivatives by metal-free catalytic hydrosilylation. Energy Environ Sci 8:2734–2743. https://doi.org/10.1039/C5EE01304F

17. Ren Y, Yan M, Wang J, et al (2013) Selective Reductive Cleavage of Inert Aryl C-O Bonds by an Iron Catalyst. Angew Chem Int Ed 52:12674–12678. https://doi.org/10.1002/anie.201305342

18. Liu Y, Li C, Miao W, et al (2019) Mild Redox-Neutral Depolymerization of Lignin with a Binuclear Rh Complex in Water. ACS Catal 9:4441–4447. https://doi.org/10.1021/acscatal.9b00669

19. Bosque I, Magallanes G, Rigoulet M, et al (2017) Redox Catalysis Facilitates Lignin Depolymerization. ACS Cent Sci 3:621–628. https://doi.org/10.1021/acscentsci.7b00140

20. vom Stein T, den Hartog T, Buendia J, et al (2015) Ruthenium-Catalyzed C-C Bond Cleavage in Lignin Model Substrates. Angew Chem Int Ed 54:5859–5863. https://doi.org/10.1002/anie.201410620

21. Fan L, Zhang Y, Liu S, et al (2017) Bio-oil from fast pyrolysis of lignin: Effects of process and upgrading parameters. Bioresource Technology 241:1118–1126. https://doi.org/10.1016/j.biortech.2017.05.129

22. Peng C, Zhang G, Yue J, Xu G (2014) Pyrolysis of lignin for phenols with alkaline additive. Fuel Processing Technology 124:212–221. https://doi.org/10.1016/j.fuproc.2014.02.025

23. Sedai B, Díaz-Urrutia C, Baker RT, et al (2011) Comparison of Copper and Vanadium Homogeneous Catalysts for Aerobic Oxidation of Lignin Models. ACS Catal 1:794–804. https://doi.org/10.1021/cs200149v

24. Magallanes G, Kärkäs MD, Bosque I, et al (2019) Selective C–O Bond Cleavage of Lignin Systems and Polymers Enabled by Sequential Palladium-Catalyzed Aerobic Oxidation and

Visible-Light Photoredox Catalysis. ACS Catal 9:2252–2260. https://doi.org/10.1021/acscatal.8b04172

25. Mottweiler J, Rinesch T, Besson C, et al (2015) Iron-catalysed oxidative cleavage of lignin and β-O-4 lignin model compounds with peroxides in DMSO. Green Chem 17:5001–5008. https://doi.org/10.1039/C5GC01306B

26. Kim SA, Kim SE, Kim YK, Jang H-Y (2020) Copper-Catalyzed Oxidative Cleavage of the C–C Bonds of β-Alkoxy Alcohols and β-1 Compounds. ACS Omega 5:31684–31691. https://doi.org/10.1021/acsomega.0c04162

27. Zhou Z, Liu M, Li C-J (2017) Selective Copper–N-Heterocyclic Carbene (Copper-NHC)-Catalyzed Aerobic Cleavage of β-1 Lignin Models to Aldehydes. ACS Catal 7:3344–3348. https://doi.org/10.1021/acscatal.7b00565

28. Sedai B, Baker RT (2014) Copper Catalysts for Selective C-C Bond Cleavage of β-O-4 Lignin Model Compounds. Adv. Synth. Catal. 356:3563–3574. https://doi.org/10.1002/adsc.201400463

29. Crestini C, Pro P, Neri V, Saladino R (2005) Methyltrioxorhenium: a new catalyst for the activation of hydrogen peroxide to the oxidation of lignin and lignin model compounds. Bioorganic & Medicinal Chemistry 13:2569–2578. https://doi.org/10.1016/j.bmc.2005.01.049

30. Gao K, Xu M, Cai C, et al (2020) Cobalt-Catalyzed Reductive C–O Bond Cleavage of Lignin β-O-4 Ketone Models via In Situ Generation of the Cobalt–Boryl Species. Org Lett 22:6055–6060. https://doi.org/10.1021/acs.orglett.0c02117

31. Huo W, Li W, Zhang M, et al (2014) Effective C–O Bond Cleavage of Lignin β-O-4 Model Compounds: A New RuHCl(CO)(PPh3)3/KOH Catalytic System. Catal Lett 144:1159–1163. https://doi.org/10.1007/s10562-014-1264-y

32. Zhou M, Tang C, Xia H, et al (2022) Ni-based MOFs catalytic oxidative cleavage of lignin models and lignosulfonate under oxygen atmosphere. Fuel 320:123993. https://doi.org/10.1016/j.fuel.2022.123993

33. Xu X, Wang H, Tan C-H, Ye X (2023) Applications of Vanadium, Niobium, and Tantalum Complexes in Organic and Inorganic Synthesis. ACS Org Inorg Au 3:74–91. https://doi.org/10.1021/acsorginorgau.2c00056

34. Langeslay RR, Kaphan DM, Marshall CL, et al (2019) Catalytic Applications of Vanadium: A Mechanistic Perspective. Chem Rev 119:2128–2191. https://doi.org/10.1021/acs.chemrev.8b00245

35. Hanson SK, Baker RT (2015) Knocking on Wood: Base Metal Complexes as Catalysts for Selective Oxidation of Lignin Models and Extracts. Acc Chem Res 48:2037–2048. https://doi.org/10.1021/acs.accounts.5b00104

36. Gazi S, Hung Ng WK, Ganguly R, et al (2015) Selective photocatalytic C–C bond cleavage under ambient conditions with earth abundant vanadium complexes. Chem Sci 6:7130–7142. https://doi.org/10.1039/C5SC02923F

37. Díaz-Urrutia C, Chen W-C, Crites C-O, et al (2015) Towards lignin valorization: comparing homogeneous catalysts for the aerobic oxidation and depolymerization of organosolv lignin. RSC Adv 5:70502–70511. https://doi.org/10.1039/C5RA15694G

38. Jiang Y-Y, Yan L, Yu H-Z, et al (2016) Mechanism of Vanadium-Catalyzed Selective C–O and C–C Cleavage of Lignin Model Compound. ACS Catal 6:4399–4410. https://doi.org/10.1021/acscatal.6b00239

39. Ma Y, Du Z, Liu J, et al (2015) Selective oxidative C–C bond cleavage of a lignin model compound in the presence of acetic acid with a vanadium catalyst. Green Chem 17:4968–4973. https://doi.org/10.1039/C5GC00645G

40. Sedai B, Díaz-Urrutia C, Baker RT, et al (2013) Aerobic Oxidation of β-1 Lignin Model Compounds with Copper and Oxovanadium Catalysts. ACS Catal 3:3111–3122. https://doi.org/10.1021/cs400636k

41. Son S, Toste FD (2010) Non-Oxidative Vanadium-Catalyzed C-O Bond Cleavage: Application to Degradation of Lignin Model Compounds. Angewandte Chemie International Edition 49:3791–3794. https://doi.org/10.1002/anie.201001293

42. Hanson SK, Baker RT, Gordon JC, et al (2010) Aerobic Oxidation of Lignin Models Using a Base Metal Vanadium Catalyst. Inorg Chem 49:5611–5618. https://doi.org/10.1021/ic100528n

43. Hanson SK, Wu R, Silks LA “Pete” (2012) C-C or C-O Bond Cleavage in a Phenolic Lignin Model Compound: Selectivity Depends on Vanadium Catalyst. Angew Chem Int Ed 51:3410–3413. https://doi.org/10.1002/anie.201107020

44. Zhang G, Scott BL, Wu R, et al (2012) Aerobic Oxidation Reactions Catalyzed by Vanadium Complexes of Bis(Phenolate) Ligands. Inorg Chem 51:7354–7361. https://doi.org/10.1021/ic3007525

45. Adão P, Costa Pessoa J, Henriques RT, et al (2009) Synthesis, Characterization, and Application of Vanadium−Salan Complexes in Oxygen Transfer Reactions. Inorg Chem 48:3542–3561. https://doi.org/10.1021/ic8017985

46. Belaid S, Benali-Baïtich O, Bouet G, Landreau A (2015) Synthesis, characterization, and biological activities of oxovanadium(IV) and cadmium(II) complexes with reduced Schiff

bases derived from N,N′-o-phenylenebis(salicylideneimine). Chemical Papers 69:. https://doi.org/10.1515/chempap-2015-0132

47. Groysman S, Sergeeva E, Goldberg I, Kol M (2005) Salophan Complexes of Group IV Metals. Eur J Inorg Chem 2005:2480–2485. https://doi.org/10.1002/ejic.200500243

48. Adão P, Maurya MR, Kumar U, et al (2009) Vanadium-salen and -salan complexes: Characterization and application in oxygen-transfer reactions. Pure and Applied Chemistry 81:1279–1296. https://doi.org/10.1351/PAC-CON-08-09-07

49. Hagen H, Barbon A, Van Faassen EE, et al (1999) Synthesis and Characterization of O,N-Chelated Vanadium(IV) Oxo Phenolate Complexes: Electronic Effect of Meta and Para Substituents on the Vanadium Center. Inorg Chem 38:4079–4086. https://doi.org/10.1021/ic9901564

50. Wu J, Kozlowski MC (2022) Catalytic Oxidative Coupling of Phenols and Related Compounds. ACS Catal 12:6532–6549. https://doi.org/10.1021/acscatal.2c00318

51. Dawes GJS, Scott EL, Le Nôtre J, et al (2015) Deoxygenation of biobased molecules by decarboxylation and decarbonylation – a review on the role of heterogeneous, homogeneous and bio-catalysis. Green Chem 17:3231–3250. https://doi.org/10.1039/C5GC00023H

52. Parker HJ, Chuck CJ, Woodman T, Jones MD (2016) Degradation of β-O-4 model lignin species by vanadium Schiff-base catalysts: Influence of catalyst structure and reaction conditions on activity and selectivity. Catalysis Today 269:40–47. https://doi.org/10.1016/j.cattod.2015.08.045